Lung inflammation promotes metastasis through neutrophil protease-mediated degradation of Tsp-1

Tina El Rayes[a,b,c,1], Raúl Catena[a,b,c,1], Sharrell Lee[a,c], Marcin Stawowczyk[a,b,c], Natasha Joshi[a,b,c], Claudia Fischbach[d], Charles A. Powell[e], Andrew J. Dannenberg[f], Nasser K. Altorki[a,c], Dingcheng Gao[a,b,c], and Vivek Mittal[a,b,c,2]

[a]Department of Cardiothoracic Surgery, Weill Cornell Medical College of Cornell University, New York, NY 10065; [b]Department of Cell and Developmental Biology, Weill Cornell Medical College of Cornell University, New York, NY 10065; [c]Neuberger Berman Lung Cancer Center, Weill Cornell Medical College of Cornell University, New York, NY 10065; [d]Nancy E. and Peter C. Meinig School of Biomedical Engineering, Cornell University, Ithaca, NY 14853; [e]Division of Pulmonary, Critical Care, and Sleep Medicine, Icahn School of Medicine at Mount Sinai, New York, NY 10029; and [f]Department of Medicine, Weill Cornell Medical College of Cornell University, New York, NY 10065

Edited by Steven M. Dubinett, University of California, Los Angeles, and accepted by the Editorial Board November 9, 2015 (received for review April 14, 2015)

Inflammation is inextricably associated with primary tumor progression. However, the contribution of inflammation to tumor outgrowth in metastatic organs has remained underexplored. Here, we show that extrinsic inflammation in the lungs leads to the recruitment of bone marrow-derived neutrophils, which degranulate azurophilic granules to release the Ser proteases, elastase and cathepsin G, resulting in the proteolytic destruction of the antitumorigenic factor thrombospondin-1 (Tsp-1). Genetic ablation of these neutrophil proteases protected Tsp-1 from degradation and suppressed lung metastasis. These results provide mechanistic insights into the contribution of inflammatory neutrophils to metastasis and highlight the unique neutrophil protease–Tsp-1 axis as a potential antimetastatic therapeutic target.

metastasis | inflammation | neutrophils | proteases | thrombospondin-1

The contribution of inflammation to primary tumor progression is well documented (1); however, little is known about its role in metastatic outgrowth in distant organs. The lung, which is a frequent site of metastasis from extrapulmonary neoplasms, is susceptible to inflammatory insults. Bacterial infection-induced, metastasis-conducive environments in the lung (2, 3) and cigarette smoke-induced inflammation were associated with pulmonary metastasis from breast cancer (2, 4).

Bacterial lipopolysaccharide (LPS) is a well-characterized inducer of inflammation because its binding to toll-like receptor 4 (TLR4) results in nuclear factor kappa B (NF-κB) activation and expression of proinflammatory cytokines, including interleukin-1 beta (IL-1β), tumor necrosis factor alpha (TNF-α), and IL-6 (5). LPS-induced acute lung injury is marked by increased neutrophil influx and up-regulation of proinflammatory cytokines. Similar phenotypes are observed in other lung inflammatory conditions, including asthma (6), chronic obstructive pulmonary disease (7), and pneumonia (8, 9). LPS-mediated lung inflammation is associated with breast and colon cancer metastasis to the lungs (10–12).

The mechanisms by which inflammation contributes to metastatic outgrowth in distant organs have remained underexplored. From a clinical perspective, although blocking primary tumor invasion and blocking dissemination are considered effective approaches in suppressing metastasis, an important question is how best to treat patients whose tumor has already metastasized. Thus, approaches are required to block tumor outgrowth in secondary organs for effective treatment of metastatic cancers. In this study, using two independent models of lung inflammation, we show enhanced recruitment of neutrophils, which degranulate to release the Ser proteases, neutrophil elastase (NE) and cathepsin G (CG), to degrade thrombospondin-1 (Tsp-1) in the lung microenvironment, enhancing metastatic outgrowth. Protease deficiency protected Tsp-1 from proteolysis and suppressed metastasis, providing a previously unidentified mechanism of Tsp-1 regulation in the metastatic organ.

Results

Neutrophil-Mediated Lung Inflammation Enhances Metastatic Outgrowth. To determine the contribution of inflammation in the lungs to the outgrowth of metastasis, we generated lung-specific inflammation through intranasal instillation of LPS. As expected, intranasal LPS administration confined the recruitment of neutrophils to the lungs and not to other organs, ruling out systemic inflammation (Fig. 1*A*). These lungs and the recruited Ly6G$^+$ neutrophils expressed potent inflammatory mediators, including IL-1β, TNF-α, IL-6, and cyclooxygenase-2 (Cox-2) (Fig. 1*B* and Fig. S1*A*). Further characterization by flow cytometry showed increased recruitment (>sevenfold) of bone marrow (BM)-derived CD45$^+$ CD11b$^+$ Ly6G$^+$ neutrophils (Fig. S1 *B* and *C*). Taken together, these data suggest that intranasal LPS administration generates an inflammatory microenvironment in the lungs characterized by an influx of neutrophils and the induction of inflammatory mediators.

To determine the consequence of lung inflammation on metastasis, we used orthotopic B16-BL6 melanoma, which metastasizes to the lungs from the skin (13). Enhanced melanoma metastasis was observed in LPS-inflamed lungs (Fig. 1*C*), associated with a marked increase in Ly6G$^+$ neutrophils (Tum-LPS) compared to controls (Tum-Ctrl) (Fig. S2*A*). These data are consistent with the findings of LPS-challenged, tumor-free mice (Fig. 1*A* and Fig. S1 *B* and *C*), and suggest an association between neutrophil recruitment and metastasis.

Having demonstrated that inflammation confined to the lung microenvironment can promote metastasis of orthotopic primary tumors, we next interrogated the molecular mechanisms by which neutrophil-mediated lung inflammation contributes to metastatic

Significance

Lungs are highly susceptible to inflammation. However, molecular insights into how external inflammation enhances metastatic outgrowth in the lungs remain lacking. Clinically, approaches are required to block tumor outgrowth in secondary organs for effective treatment of metastatic cancers. We demonstrate a previously unidentified mechanism of thrombospondin-1 (Tsp-1) regulation by inflammatory neutrophil proteases in the metastatic organ. Our findings suggest the potential of using neutrophil protease inhibitors as antimetastatic therapies.

Author contributions: T.E.R., R.C., D.G., and V.M. designed research; T.E.R., R.C., S.L., M.S., and N.J. performed research; C.F., C.A.P., A.J.D., and N.K.A. contributed new reagents/analytic tools; T.E.R., R.C., S.L., M.S., and N.J. analyzed data; T.E.R., R.C., D.G., and V.M. wrote the paper; and C.F., C.A.P., A.J.D., and N.K.A. contributed to experimental design.

The authors declare no conflict of interest.

This article is a PNAS Direct Submission. S.M.D. is a guest editor invited by the Editorial Board.

[1]T.E.R. and R.C. contributed equally to this work.

[2]To whom correspondence should be addressed. Email: vim2010@med.cornell.edu.

This article contains supporting information online at www.pnas.org/lookup/suppl/doi:10.1073/pnas.1507294112/-/DCSupplemental.

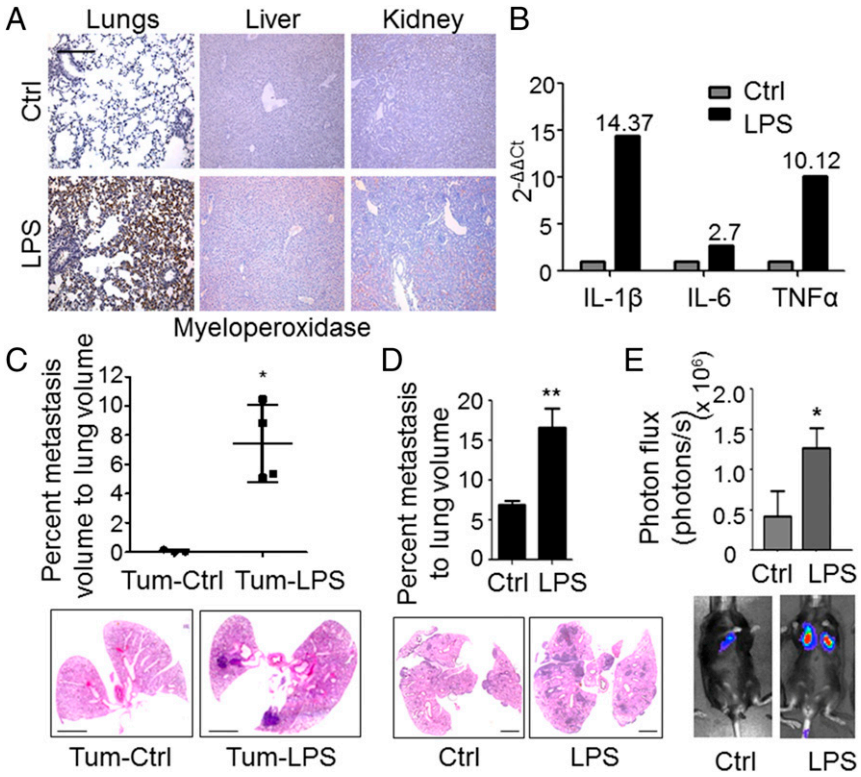

Fig. 1. Intranasal LPS administration up-regulates neutrophil recruitment and enhances metastasis to the lung. (*A*) Representative immunohistochemistry of myeloperoxidase (brown) in PBS-treated control (Ctrl) or LPS-treated mouse lung, liver, and kidney ($n = 5$ mice per group, four sections per mouse, 7–10 fields per section). (Scale bar: 100 μm.) (*B*) Representative quantitative RT-PCR depicting the normalized fold expression of the proinflammatory cytokines IL-1β, IL-6, and TNF-α in LPS-challenged lungs compared with control PBS-challenged lungs. (*C*, *Top*) Stereological quantitation of metastasis in lungs of PBS-challenged (Tum-Ctrl) or LPS-challenged (Tum-LPS) mice 6 wk after primary tumor inoculation in the skin. Data are represented as the mean ± SD ($n = 3$ Ctrl mice and $n = 4$ LPS mice, five to eight sections per lung). $*P = 0.025$ (one-tailed Mann–Whitney *U* test). (*C*, *Bottom*) Representative H&E stains of lungs. (Scale bars: 2 mm.) (*D*, *Top*) Stereological quantitation of B16-BL6 melanoma lung metastases in Ctrl or LPS-challenged mice 18 d following tail vein injection of 2×10^5 B16-BL6 cells. Data are plotted as the mean ± SEM ($n = 10$ mice per group). $**P = 0.002$ (one-tailed *t* test with Welch's correction). (*D*, *Bottom*) Representative H&E stains. (Scale bars: 2 mm.) (*E*, *Top*) Quantitation using bioluminescence imaging (BLI) of LLC pulmonary metastases in Ctrl or LPS-challenged mice 15 d following tail vein injection of 1×10^5 LLC cells. Data are plotted as the mean ± SEM ($n = 5$ mice per group, similar data in two repeat experiments). $*P = 0.048$ (one-tailed Mann–Whitney *U* test). (*E*, *Bottom*) Representative BLI images.

outgrowth. However, the orthotopic tumor model is not optimal to interrogate mechanisms, since primary tumors systemically generate BM-derived premetastatic niches with inflammatory characteristics in metastatic organs (14–16). Consistent with this notion, lungs of tumor-bearing mice (Tum-Ctrl) showed increased $CD45^+$ cell content (Fig. S2*B*), suggesting that an experimental metastasis model is necessary to circumvent the confounding effects of primary tumor-generated lung inflammation. Importantly, LPS-inflamed lungs showed an increased metastatic burden following i.v. administration of melanoma cells (Fig. 1*D*). Similarly, Lewis lung carcinoma (LLC) cells, widely used in metastasis studies (17, 18), also showed increased lung metastasis following LPS challenge (Fig. 1*E*), suggesting that lung inflammation has an impact on metastasis across tumor types. Importantly, there was no significant difference in the number of cells that extravasate or seed in LPS-conditioned lungs compared with controls (Fig. S3), suggesting that the differences in lung tumor burden observed are due to enhanced tumor initiation or outgrowth after initial seeding. Importantly, neutrophil depletion with anti-Ly6G neutralizing Ab (19) reduced lung metastasis (Fig. S4), confirming the specific and dominant contribution of neutrophils to the inflammation-mediated metastatic phenotype.

Inflamed Lungs Show Loss of Tsp-1 and Up-Regulation of Neutrophil Ser Protease Activity. To elucidate the mechanisms by which neutrophils in the inflamed lungs promote metastasis, we focused on Tsp-1, a secreted ECM protein critical for lung homeostasis and inflammation (20, 21). Tsp-1 deficiency extends inflammation and confers worse lung fibrosis in response to bleomycin treatment (22). Furthermore, we had previously demonstrated that myeloid cell-derived Tsp-1 contributes to lung metastasis suppression (23). Analysis of inflamed lungs showed loss of Tsp-1 protein compared with controls (Fig. 2*A*). Given that Tsp-1 is a potent inhibitor of tumor angiogenesis and growth (24, 25), we posited that decreased Tsp-1 protein may enhance metastasis. The loss of Tsp-1 protein was not due to a reduction in neutrophil Tsp-1 mRNA levels (Fig. 2*B*), suggesting posttranslational regulation of Tsp-1, and potentially, proteolytic degradation by neutrophil proteases. Of note, the trend of increased neutrophil Tsp-1 mRNA in LPS-inflamed lungs can be attributed to the activation of neutrophil transcription by inflammation (26).

Neutrophils carry Ser proteases, among which NE and CG have binding affinity for Tsp-1 (27). Given that NE and CG are stored in specialized azurophilic granules, and inflammation is a major trigger of neutrophil degranulation (28), we speculated that degranulating neutrophils in the inflamed lungs, by virtue of secreting NE and CG, may mediate Tsp-1 proteolysis. Indeed, increased neutrophil degranulation was detected in inflamed lungs, as determined by cell surface presentation of the azurophilic granule membrane molecule CD63 (29) (Fig. 2*C*). Increased neutrophil degranulation was associated with enhanced activity of both NE and CG in inflamed lungs (Fig. 2*D*).

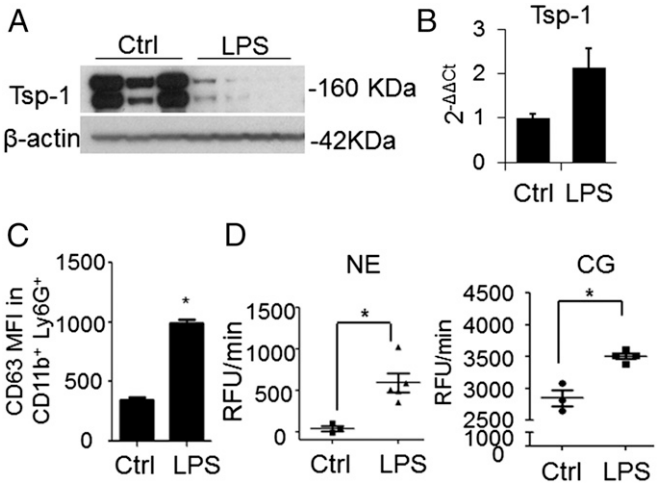

Fig. 2. Neutrophil recruitment in LPS-inflamed lungs is associated with Tsp-1 degradation. (*A*) Western blot analysis of Tsp-1 levels in the lungs of WT mice challenged with PBS (Ctrl, $n = 3$ mice) or LPS ($n = 4$ mice). β-Actin was used as a loading control. The experiment was reproduced three times with comparable results. (*B*) Quantitative RT-PCR analysis of Tsp-1 in flow cytometry-sorted Ly6G$^+$ cells from the lungs of PBS-challenged (Ctrl) or LPS-challenged mice. Samples were normalized based on equal Ly6G$^+$ cell numbers, and normalized to GAPDH mRNA. Data are plotted as the mean ± SEM ($n = 3$ mice per group, in duplicates). The PBS group was used as a control for relative expression ($2^{-\Delta\Delta Ct}$). (*C*) Flow cytometry analysis of CD63 median fluorescence intensity (MFI) in the CD11b$^+$ Ly6G$^+$ population in lungs of control and LPS-challenged mice. Data are plotted as the mean ± SEM ($n = 4$ mice per group). *$P = 0.029$ (one-tailed Mann–Whitney *U* test). The experiment was reproduced twice with comparable results. (*D*) NE activity (*Left*) and CG activity (*Right*) in lungs of PBS-treated (Ctrl) and LPS-treated mice. Activity is presented as relative fluorescence units per minute (RFU/min) and plotted as the mean ± SEM ($n = 4$ mice per group). *$P = 0.018$ and *$P = 0.029$ for NE activity and CG activity, respectively (one-tailed Mann–Whitney *U* test).

To determine that the mechanisms identified above are not confined to the LPS model of inflammation, we evaluated a genetic model of inflammation, Clara cell secretory protein (CCSP)–tetracycline-controlled transactivator (rtTA); tetO–IL-1β, where the potent inflammatory cytokine IL-1β is conditionally expressed in the lung epithelium, under the CCSP promoter (30). Consistent with the LPS model, conditional expression of IL-1β increased the recruitment of Ly6G$^+$ neutrophils, elevated the levels of proinflammatory mediators, and induced a significant increase in NE and CG activities associated with degradation of Tsp-1 protein (Fig. 3 *A–D* and Fig. S5*A*). This phenotype translated to an enhanced metastatic burden in lungs following tail vein administration of tumor cells (Fig. 3*E* and Fig. S5*B*).

NE and CG Degrade Tsp-1 in Vitro. To show that NE and CG possess Tsp-1 proteolysis activity, we performed in vitro assays. Both NE and CG degraded recombinant Tsp-1, which was blocked in the presence of protease-specific inhibitors (Fig. 4 *A* and *B*). We also tested sivelestat (ONO-5046), a pharmacological inhibitor of NE ($IC_{50} = 44$ nM, $K_i = 0.2$ μM), used for treatment of acute lung injury in animals (31, 32), and humans (33). As expected, sivelestat inhibited NE-mediated Tsp-1 proteolysis (Fig. 4*A*). Strikingly, we found that sivelestat also reduced CG-mediated Tsp-1 proteolysis (Fig. 4*B*), thereby exhibiting dual protease inhibitor activity. This dual activity can be explained by structural homology and a conserved catalytic triad in these proteases (34). To expand upon the role of neutrophils in Tsp-1 proteolysis through degranulation of proteases, we isolated neutrophils and induced degranulation with the phorbol ester 12-O-tetradecanoylphorbol-13-acetate (TPA) (35). TPA-induced neutrophil degranulation was confirmed by the membrane presentation of CD63 (Fig. 4*C*). Conditioned media (CM) from TPA-treated neutrophils showed an increase in NE and CG protease activity (Fig. 4*D*) and induced Tsp-1 proteolysis (Fig. 4*E*). Notably, sivelestat concurrently blocked NE and CG protease activity in the CM and protected Tsp-1 from proteolysis (Fig. 4 *D* and *E*) without inhibiting neutrophil degranulation (Fig. 4*C*).

NE and CG Degrade Tsp-1 in Vivo. To demonstrate the causal relationship between NE and CG release from neutrophils and the degradation of Tsp-1, we used Ly6G$^+$ neutrophils harvested from the BM of NE$^{-/-}$ CG$^{-/-}$ mice. NE$^{-/-}$ CG$^{-/-}$ neutrophils showed similar degrees of degranulation as WT neutrophils following TPA treatment (Fig. 5*A*). As expected, NE$^{-/-}$ CG$^{-/-}$ neutrophils lacking CG and NE activity (Fig. 5*B*) failed to induce Tsp-1 degradation (Fig. 5*C*). In vivo, LPS-induced lung inflammation showed Tsp-1 degradation in WT mice, as expected; however, strikingly, lungs of NE$^{-/-}$ CG$^{-/-}$ mice showed protection of Tsp-1 from proteolysis (Fig. 5*D*), a phenotype not attributed to defects in degranulation (Fig. 5*E*).

Taken together, these data suggest that neutrophil proteases NE and CG mediate Tsp-1 proteolysis both in vitro and in vivo, highlighting a previously unidentified mechanism of Tsp-1 regulation by the combined proteolytic activity of NE and CG.

NE and CG Activities Are Required for Inflammation-Enhanced Metastasis. To determine the contribution of the NE/CG–Tsp-1 axis in promoting metastasis, we generated NE and CG deficiency. To ensure that the protease deficiency is confined specifically to the BM cells in the inflamed lungs, a bone marrow transplantation (BMT) approach was used. Specifically, BM cells harvested from NE$^{-/-}$ CG$^{-/-}$ mice were transplanted into irradiated syngeneic WT mice to generate a cohort of NE$^{-/-}$ CG$^{-/-}$ BMT mice. As controls, BM from WT mice was transplanted into irradiated WT mice, generating WT BMT mice. Importantly, NE and CG deficiency in BM cells in NE$^{-/-}$ CG$^{-/-}$ BMT mice did not perturb the mobilization, recruitment, or degranulation of neutrophils after LPS treatment (Fig. S6 *B–D*). Moreover, deficiency of NE and CG did not have an impact on hematopoietic cell subsets (Fig. S6*A*). Strikingly, impaired lung metastasis was observed after LPS challenge in NE$^{-/-}$ CG$^{-/-}$ BMT mice compared with WT BMT mice (Fig. 5*F*). Western blot analysis of the total lung lysates showed protection of Tsp-1 from proteolysis in NE$^{-/-}$ CG$^{-/-}$ BMT mice compared with WT BMT controls (Fig. 5*G*). Deficiency of either NE or CG only partially suppressed metastasis (Fig. S6 *E* and *F*), consistent with the ability of both of these proteases to degrade Tsp-1. Taken together, these results suggest the contribution of the NE/CG–Tsp-1 axis to inflammation-driven metastasis.

Discussion

Primary tumors systemically induce metastasis-promoting microenvironments referred to as the "premetastatic niche" in distant organs (36). These microenvironments are composed of a variety of BM-derived cellular populations and exhibit inflammatory features (14, 15). Identifying mechanisms by which tumor-derived premetastatic niches contribute to tumor outgrowth is an area of active investigation; however, little is known about the mechanisms by which extrinsic inflammation in the lungs can influence metastasis of extrapulmonary neoplasms. We have described a previously unidentified mechanism, whereby neutrophils recruited in large numbers to the inflamed lungs degranulate and release stored proteases. These proteases specifically target a potent antitumorigenic factor, Tsp-1, resulting in its degradation. This mechanism appears to be responsible for the enhanced metastatic phenotype observed in inflamed lungs (Fig. 6), since deleting both NE and CG in the BM compartment suppresses metastasis. However, future studies using NE$^{-/-}$ CG$^{-/-}$ Tsp-1$^{-/-}$ triple-KO mice are required to

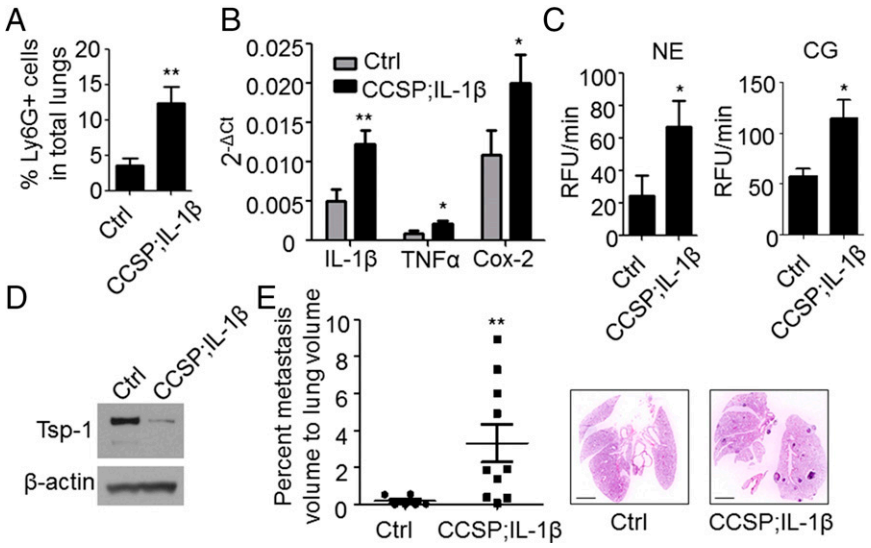

Fig. 3. Conditional expression of IL-1β in lungs promotes neutrophil recruitment, Tsp-1 degradation, and enhanced metastatic outgrowth. (*A*) Flow cytometry-based quantification of Ly6G$^+$ cells in lungs of CCSP–tetracycline-controlled transactivator (rtTA); tetO–IL-1β or age-matched control littermates (WT or CCSP-rtTA single-transgenic) administered doxycycline for 10 d ($n = 5$ controls and $n = 7$ CCSP-rtTA; tetO–IL-1β). $^{**}P = 0.0064$ (one-tailed *t* test). Data are represented as the mean ± SEM. (*B*) Representative quantitative RT-PCR depicting the normalized expression of the proinflammatory mediators IL-1β, TNF-α, and Cox-2 in lungs of CCSP-rtTA; tetO–IL-1β mice and controls administered doxycycline for 10 d ($n = 5$ controls and $n = 7$ CCSP-rtTA; tetO-IL-1β). $^{**}P = 0.005$ and $^{*}P = 0.025$ for IL-1β and TNF-α, respectively (one-tailed *t* test). $^{*}P = 0.014$ for Cox-2 (one-tailed Mann–Whitney *U* test). Data are represented as the mean ± SEM. (*C*) NE activity (*Left*) and CG activity (*Right*) in lungs of CCSP-rtTA; tetO–IL-1β mice and controls administered doxycycline for 10 d ($n = 5$ controls and $n = 7$ CCSP-rtTA; tetO–IL-1β). Activity is represented as RFU/min. $^{*}P = 0.038$ and $^{*}P = 0.013$ for NE and CG activity, respectively (one-tailed *t* test). Data are represented as the mean ± SEM. (*D*) Western blot analysis of Tsp-1 in pooled lungs of bitransgenic mice or littermates administered doxycycline for 10 d ($n = 5$ controls and $n = 7$ CCSP-rtTA; tetO–IL-1β). β-Actin is used as a loading control. (*E*, *Left*) Stereological measurements of lung metastases 28 d after tail vein injection of 1×10^6 mouse mammary tumor virus-polyoma middle T antigen (MMTV-PyMT) (FVB/N strain)–derived breast cancer single-cell suspensions into syngeneic CCSP-rtTA; tetO–IL-1β or age-matched control littermates (FVB/N strain) that were administered doxycycline for 8 d. Data are plotted as the mean ± SEM ($n = 6$ controls and $n = 10$ CCSP-rtTA; tetO–IL-1β). $^{**}P = 0.005$ (one-tailed Mann–Whitney *U* test). (*E*, *Right*) Representative H&E stains. (Scale bars: 2 mm.)

establish firmly the causal link between the NE/CG–Tsp-1 axis and metastasis.

The finding that NE and CG can degrade Tsp-1 and have an impact on its antitumorigenic function is unique, since previous studies have demonstrated that specific Tsp-1 cleavage contributes to Tsp-1 function. A disintegrin and metalloproteinase with thrombospondin motifs 1 (ADAM-TS1)–mediated cleavage of Tsp-1 was shown to release a C-terminal 110-kDa antiangiogenic fragment from matrix-bound Tsp-1 (37). In another study, thrombin was shown to cleave Tsp-1 to release a 25-kDa N-terminal heparin-binding

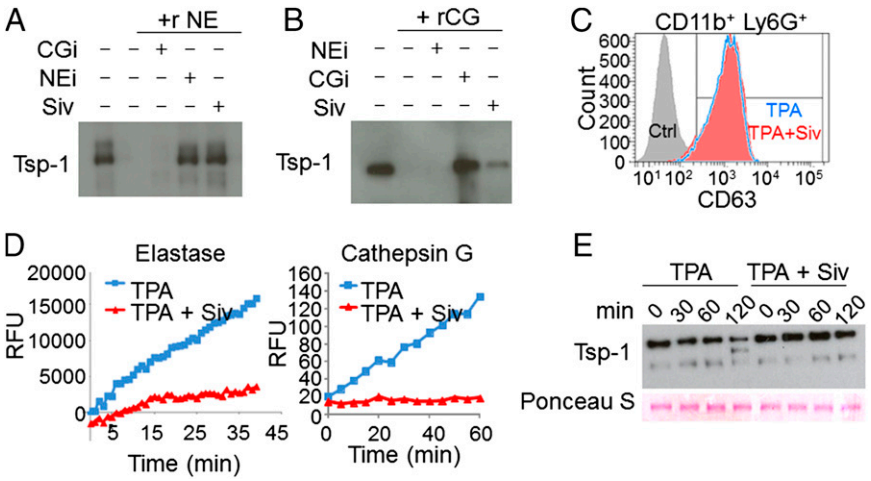

Fig. 4. Neutrophil-derived Ser proteases mediate proteolysis of Tsp-1. (*A* and *B*) In vitro degradation assays of recombinant Tsp-1 with recombinant NE and CG proteases, alone or in combination with the specific inhibitors of NE or CG, and sivelestat. Recombinant (r) protein incubations were followed by Western blot analysis for Tsp-1 levels. Experiments were repeated three times with similar results. (*C*) Representative flow cytometry analysis of degranulation marker CD63 in CD11b$^+$ Ly6G$^+$ cells cultured in vitro with 0.01% DMSO (Ctrl, solid gray histogram), 20 nM TPA (TPA, empty blue histogram), or 20 nM TPA + 0.05 μg/μL sivelestat (Siv, solid red histogram). Experiments were repeated three times with similar results. (*D*) Representative protease activity assays for NE (*Left*) and CG (*Right*) in CM of Ly6G$^+$ cells cultured in vitro with 20 nM TPA or 20 nM TPA + 0.05 μg/μL Siv. Activities are represented as RFUs as a function of time. Experiments were repeated twice with similar results. (*E*) Western blot analysis of Tsp-1 in CM of Ly6G$^+$ cells cultured in the presence of TPA or TPA + Siv at $t = 0$, 30, 60, and 120 min. Ponceau S staining shows equal protein loading.

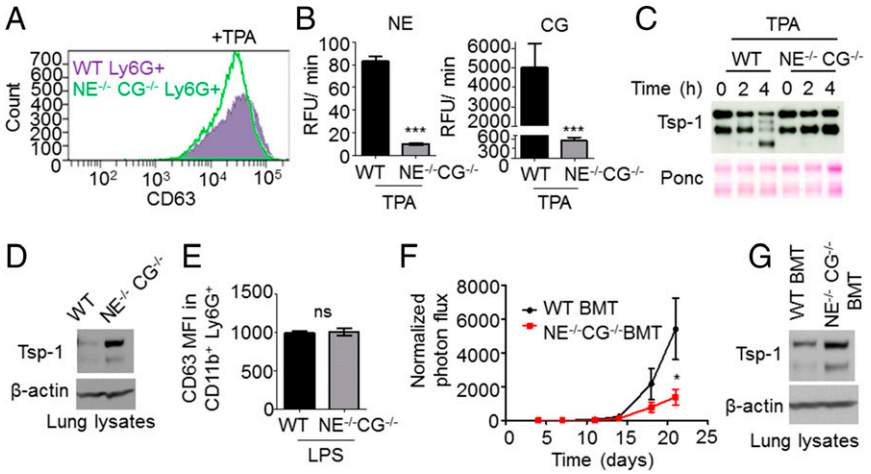

Fig. 5. Neutrophil Ser proteases NE and CG work in concert to degrade Tsp-1 and enhance metastasis. (*A*) Representative flow cytometry analysis of the degranulation marker CD63, in CD11b$^+$ Ly6G$^+$ cells isolated from WT mouse lungs (solid purple histogram) and NE$^{-/-}$ CG$^{-/-}$ mouse lungs (empty green histogram) and cultured in vitro with 20 nM TPA. Experiments were repeated three times with similar results. (*B*) NE activity (*Left*) and CG activity (*Right*) in CM of Ly6G$^+$ cells isolated from WT and NE$^{-/-}$ CG$^{-/-}$ mouse BM and cultured with 20 nM TPA for 30 min. Data are plotted as the mean ± SEM (n = 3 per group). ***$P < 0.001$ for NE activity and for CG activity [analysis of covariance (ANCOVA), comparing activity curves]. (*C*) Representative Western blot analysis of Tsp-1 in CM from Ly6G$^+$ cells isolated from WT and NE$^{-/-}$ CG$^{-/-}$ mouse BM and cultured with 20 nM TPA for t = 0, 2, or 4 h. Ponceau S (Ponc) staining is used as a loading control. Experiments were repeated twice with similar results. (*D*) Western blot analysis of Tsp-1 protein in lungs of WT and NE$^{-/-}$ CG$^{-/-}$ mice treated with LPS. Protein samples are pooled from four mice per group. β-Actin serves as a loading control. (*E*) Flow cytometry analysis of the MFI of the degranulation marker CD63 in CD11b$^+$ Ly6G$^+$ cells in lungs of WT and NE$^{-/-}$ CG$^{-/-}$ mice treated with LPS. Data are plotted as the mean ± SEM (n = 4 lungs per group). ns, not significant (two-tailed Mann–Whitney U test). (*F*) Quantification of metastatic burden via BLI in WT BMT and NE$^{-/-}$ CG$^{-/-}$ BMT mice treated with LPS and tail vein injected with LLC tumor cells. Signals were normalized to the readings obtained at day 4 for each individual animal. Data at each time point are plotted as the mean ± SEM (n = 8 mice per group). *$P = 0.038$ at day 21 (one-tailed t test with Welch's correction). (*G*) Western blot analysis of Tsp-1 in lung samples from WT BMT and NE$^{-/-}$ CG$^{-/-}$ BMT mice treated with LPS. Samples are pooled from three mice per group. β-Actin serves as a loading control.

fragment (38). Furthermore, a 140-kDa C-terminal fragment of Tsp-1 released by thrombin was shown to sequester basic FGF, hence inhibiting endothelial cell proliferation (39). In our study, none of these products appeared in the inflamed lungs of mice (Fig. S7), suggesting a novel mechanism of Tsp-1 regulation by the combined proteolytic activity of NE and CG.

LPS-inflamed lungs also showed changes in the recruitment of other cell populations (Fig. S1 *B* and *C*), which may also contribute to metastasis. However, our focus was to evaluate the most significant increase in neutrophil recruitment, since these cells are critical players in inflammation. Importantly, neutrophil depletion conferred a dramatic antimetastatic phenotype (Fig. S4), suggesting that in the context of inflammation, the neutrophils exert a specific and dominant effect on metastasis. Furthermore, knocking out both neutrophil-restricted proteases, NE and CG, significantly impaired metastasis (Fig. 5*F*).

Our study also provides insights into the exquisite functional plasticity of the Ly6G$^+$ cells, because they are the main source of both the proteases and the substrate, Tsp-1, in the lungs (23). Under normal physiological conditions, these neutrophils produce intact functional Tsp-1 that confers a tumor-inhibitory microenvironment. However, under inflammatory conditions, the same neutrophils antagonize the antimetastatic effect of Tsp-1 by degranulating and releasing NE and CG proteases. Such plasticity of neutrophils has been previously described in primary tumors, where TGF-β can drive neutrophils toward a protumorigenic "N2" phenotype (40, 41). Paradoxically, tumor-entrained neutrophils that are recruited to the premetastatic lungs have been shown to block metastatic seeding (42). In our study, the inflammatory neutrophils have not been entrained by tumor cells but merely respond to external inflammation-promoting insults. Tsp-1 degradation is a consequence of this response, which inevitably renders the lung microenvironment more conducive to tumor outgrowth. Strikingly, mouse mammary tumor virus-polyoma middle T antigen (MMTV-PyMT) mice with primary breast tumors generated a premetastatic niche in the lungs with abundant neutrophil infiltration associated with a conspicuous loss of Tsp-1 protein (Fig. S8), suggesting that primary tumors can generate an inflammation-like, Tsp-1–deficient microenvironment in the lungs.

From the perspective of targeting metastases, it has been emphasized that therapy should be targeted not only against tumor

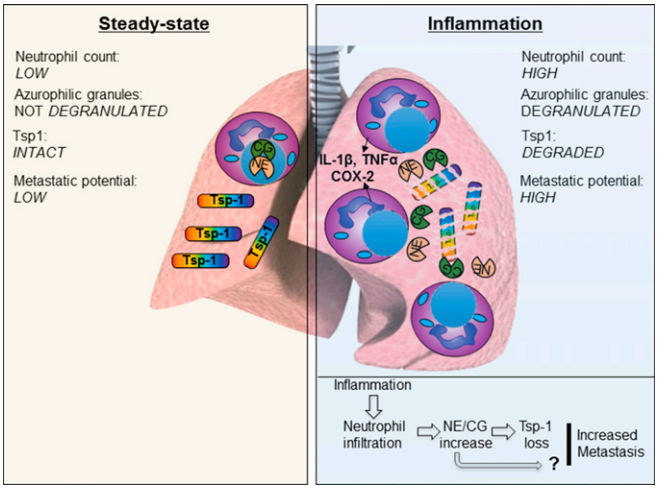

Fig. 6. Proposed model of inflammation-enhanced metastasis. Under normal physiological conditions (steady state), lungs exhibit sparse neutrophil counts and abundant intact and functional Tsp-1. Inflammation in the lungs causes enhanced influx of BM-derived neutrophils, which are the first responders at the infection site. Activated neutrophils produce potent inflammatory mediators, including IL-1β, TNF-α, IL-6, and Cox-2, and they degranulate their azurophilic granules, releasing the Ser proteases NE and CG. NE and CG degrade Tsp-1, rendering the lung microenvironment conducive to increased metastatic outgrowth. Whether CG and NE also have a non–Tsp-1–mediated role in metastasis is not known and is depicted by a "?".

cells but also against the host microenvironment, which contributes to, and supports, the progressive growth and survival of metastatic cancer cells (43). Insight from our studies suggests that targeting neutrophils may not be a viable strategy because it may neutralize the antimetastatic effects of neutrophil-derived Tsp-1 in the microenvironment. However, we believe that targeting the neutrophil NE/CG–Tsp-1 axis may have clinical value in the prevention of metastasis or inhibition of its outgrowth.

Materials and Methods

A detailed description of materials and methods can be found in *SI Materials and Methods*. All animal work was conducted in accordance with a protocol approved by the Institutional Animal Care and Use Committee at Weill Cornell Medical College.

BM Isolation and BMT. BMT was performed by injecting 1×10^7 total BM cells retroorbitally into lethally irradiated (900 rad), 8-wk-old C57BL/6 female mice.

LPS Treatments. LPS derived from *Escherichia coli* strain 0111:B4 was administered intranasally in a 50-μL volume at a concentration of 0.25 mg/mL on days 0, 3, and 7.

Metastasis Assay, Bioluminescence Imaging, and Analysis. For experimental metastasis, 8-wk-old C57BL/6 mice were injected via the tail vein with 5×10^5 luciferase-labeled LLC cells or 2×10^5 B16-BL6 unlabeled melanoma cells. LLC pulmonary metastases were monitored by live animal bioluminescence imaging, where mice were anesthetized and injected retroorbitally with 75 mg/kg of D-luciferin in 50 μL total volume.

Neutrophil Isolation, Culture, and Degranulation. BM cells were subjected to magnetic bead isolation using an anti-Ly6G microbead kit (MACS; Miltenyi Biotec). $Ly6G^+$ cells were cultured for 30 min at 37 °C in DMSO vehicle (final concentration of 0.01% DMSO) or 20 nM TPA.

NE and CG Activity Assays. NE activity was measured using an EnzChek Elastase assay kit (Molecular Probes) according to the manufacturer's protocol, and CG was measured using a Sensolyte 520 Cathepsin G assay kit (AnaSpec) according to the manufacturer's protocol.

ACKNOWLEDGMENTS. We thank Dr. Hyejin Choi and Dr. Kari Fischer for comments. Support from the Cornell Center on the Microenvironment and Metastasis (Grant U54CA14387 to V.M. and C.F.) and the National Lung Cancer Partnership (R.C. and D.G.) is recognized. R.C. was supported by fellowships from the "Government of Navarra" and the "Camara Navarra de Comercio" (Spain).

1. Ben-Neriah Y, Karin M (2011) Inflammation meets cancer, with NF-κB as the matchmaker. *Nat Immunol* 12(8):715–723.
2. Murin S, Pinkerton KE, Hubbard NE, Erickson K (2004) The effect of cigarette smoke exposure on pulmonary metastatic disease in a murine model of metastatic breast cancer. *Chest* 125(4):1467–1471.
3. Smith HA, Kang Y (2013) Acute infection induces a metastatic niche: A double menace for cancer patients. *Clin Cancer Res* 19(17):4547–4549.
4. Murin S, Inciardi J (2001) Cigarette smoking and the risk of pulmonary metastasis from breast cancer. *Chest* 119(6):1635–1640.
5. Takeuchi O, Akira S (2010) Pattern recognition receptors and inflammation. *Cell* 140(6):805–820.
6. Fahy JV (2009) Eosinophilic and neutrophilic inflammation in asthma: Insights from clinical studies. *Proc Am Thorac Soc* 6(3):256–259.
7. Jeffery PK (1998) Structural and inflammatory changes in COPD: A comparison with asthma. *Thorax* 53(2):129–136.
8. Craig A, Mai J, Cai S, Jeyaseelan S (2009) Neutrophil recruitment to the lungs during bacterial pneumonia. *Infect Immun* 77(2):568–575.
9. Yamamoto K, et al. (2014) Roles of lung epithelium in neutrophil recruitment during pneumococcal pneumonia. *Am J Respir Cell Mol Biol* 50(2):253–262.
10. Yan L, Cai Q, Xu Y (2013) The ubiquitin-CXCR4 axis plays an important role in acute lung infection-enhanced lung tumor metastasis. *Clin Cancer Res* 19(17):4706–4716.
11. Luo J-L, Maeda S, Hsu L-C, Yagita H, Karin M (2004) Inhibition of NF-kappaB in cancer cells converts inflammation-induced tumor growth mediated by TNFalpha to TRAIL-mediated tumor regression. *Cancer Cell* 6(3):297–305.
12. Jiang M, et al. (2014) Systemic inflammation promotes lung metastasis via E-selectin upregulation in mouse breast cancer model. *Cancer Biol Ther* 15(6):789–796.
13. Nakamura K, et al. (2002) Characterization of mouse melanoma cell lines by their mortal malignancy using an experimental metastatic model. *Life Sci* 70(7):791–798.
14. Psaila B, Lyden D (2009) The metastatic niche: Adapting the foreign soil. *Nat Rev Cancer* 9(4):285–293.
15. Hiratsuka S, et al. (2008) The S100A8-serum amyloid A3-TLR4 paracrine cascade establishes a pre-metastatic phase. *Nat Cell Biol* 10(11):1349–1355.
16. Gao D, et al. (2012) Myeloid progenitor cells in the premetastatic lung promote metastases by inducing mesenchymal to epithelial transition. *Cancer Res* 72(6):1384–1394.
17. Kim S, et al. (2009) Carcinoma-produced factors activate myeloid cells through TLR2 to stimulate metastasis. *Nature* 457(7225):102–106.
18. Gao D, et al. (2008) Endothelial progenitor cells control the angiogenic switch in mouse lung metastasis. *Science* 319(5860):195–198.
19. Daley JM, Thomay AA, Connolly MD, Reichner JS, Albina JE (2008) Use of Ly6G-specific monoclonal antibody to deplete neutrophils in mice. *J Leukoc Biol* 83(1):64–70.
20. Lawler J, et al. (1998) Thrombospondin-1 is required for normal murine pulmonary homeostasis and its absence causes pneumonia. *J Clin Invest* 101(5):982–992.
21. Lopez-Dee Z, Pidcock K, Gutierrez LS (2011) Thrombospondin-1: Multiple paths to inflammation. *Mediators Inflamm* 2011:296069.
22. Ezzie ME, et al. (2011) Thrombospondin-1-deficient mice are not protected from bleomycin-induced pulmonary fibrosis. *Am J Respir Cell Mol Biol* 44(4):556–561.
23. Catena R, et al. (2013) Bone marrow-derived Gr1+ cells can generate a metastasis-resistant microenvironment via induced secretion of thrombospondin-1. *Cancer Discov* 3(5):578–589.
24. Good DJ, et al. (1990) A tumor suppressor-dependent inhibitor of angiogenesis is immunologically and functionally indistinguishable from a fragment of thrombospondin. *Proc Natl Acad Sci USA* 87(17):6624–6628.
25. Lawler J (2002) Thrombospondin-1 as an endogenous inhibitor of angiogenesis and tumor growth. *J Cell Mol Med* 6(1):1–12.
26. Barnes PJ, Karin M (1997) Nuclear factor-kappaB: A pivotal transcription factor in chronic inflammatory diseases. *N Engl J Med* 336(15):1066–1071.
27. Hogg PJ, Jiménez BM, Chesterman CN (1994) Identification of possible inhibitory reactive centers in thrombospondin 1 that may bind cathepsin G and neutrophil elastase. *Biochemistry* 33(21):6531–6537.
28. Faurschou M, Borregaard N (2003) Neutrophil granules and secretory vesicles in inflammation. *Microbes Infect* 5(14):1317–1327.
29. Kuijpers TW, et al. (1991) Membrane surface antigen expression on neutrophils: A reappraisal of the use of surface markers for neutrophil activation. *Blood* 78(4):1105–1111.
30. Lappalainen U, Whitsett JA, Wert SE, Tichelaar JW, Bry K (2005) Interleukin-1β causes pulmonary inflammation, emphysema, and airway remodeling in the adult murine lung. *Am J Respir Cell Mol Biol* 32(4):311–318.
31. Hagio T, et al. (2004) Elastase inhibition reduced death associated with acid aspiration-induced lung injury in hamsters. *Eur J Pharmacol* 488(1-3):173–180.
32. Hagio T, Matsumoto S, Nakao S, Matsuoka S, Kawabata K (2005) Sivelestat, a specific neutrophil elastase inhibitor, prevented phorbol myristate acetate-induced acute lung injury in conscious rabbits. *Pulm Pharmacol Ther* 18(4):285–290.
33. Iwata K, et al. (2010) Effect of neutrophil elastase inhibitor (sivelestat sodium) in the treatment of acute lung injury (ALI) and acute respiratory distress syndrome (ARDS): A systematic review and meta-analysis. *Intern Med* 49(22):2423–2432.
34. Averhoff P, Kolbe M, Zychlinsky A, Weinrauch Y (2008) Single residue determines the specificity of neutrophil elastase for Shigella virulence factors. *J Mol Biol* 377(4):1053–1066.
35. Grinstein S, Furuya W (1986) Cytoplasmic pH regulation in activated human neutrophils: effects of adenosine and pertussis toxin on Na+/H+ exchange and metabolic acidification. *Biochim Biophys Acta* 889(3):301–309.
36. Joyce JA, Pollard JW (2009) Microenvironmental regulation of metastasis. *Nat Rev Cancer* 9(4):239–252.
37. Lee NV, et al. (2006) ADAMTS1 mediates the release of antiangiogenic polypeptides from TSP1 and 2. *EMBO J* 25(22):5270–5283.
38. Lawler J, Connolly JE, Ferro P, Derick LH (1986) Thrombin and chymotrypsin interactions with thrombospondin. *Ann N Y Acad Sci* 485:273–287.
39. Taraboletti G, et al. (1997) The 140-kilodalton antiangiogenic fragment of thrombospondin-1 binds to basic fibroblast growth factor. *Cell Growth Differ* 8(4):471–479.
40. Fridlender ZG, et al. (2009) Polarization of tumor-associated neutrophil phenotype by TGF-beta: "N1" versus "N2" TAN. *Cancer Cell* 16(3):183–194.
41. Fridlender ZG, Albelda SM (2012) Tumor-associated neutrophils: Friend or foe? *Carcinogenesis* 33(5):949–955.
42. Granot Z, et al. (2011) Tumor entrained neutrophils inhibit seeding in the premetastatic lung. *Cancer Cell* 20(3):300–314.
43. Fidler IJ (2003) The pathogenesis of cancer metastasis: The 'seed and soil' hypothesis revisited. *Nat Rev Cancer* 3(6):453–458.
44. Nielsen BS, et al. (2001) A precise and efficient stereological method for determining murine lung metastasis volumes. *Am J Pathol* 158(6):1997–2003.